SCIENCE CHINA
Earth Sciences

• RESEARCH PAPER •

December 2014 Vol.57 No.12: 2922–2927
doi: 10.1007/s11430-014-4980-7

Trace element composition in tuite decomposed from natural apatite in high-pressure and high-temperature experiments

ZHAI ShuangMeng[1,2*], XUE WeiHong[1], Daisuke YAMAZAKI[3] & MA Fang[2]

[1] *Key Laboratory of High-temperature and High-pressure Study of the Earth's Interior, Institute of Geochemistry, Chinese Academy of Sciences, Guiyang, 550002, China;*
[2] *School of Earth and Space Sciences, Peking University, Beijing 100871, China;*
[3] *Institute for Study of the Earth's Interior, Okayama University, Misasa 682-0193, Japan*

Received November 14, 2013; accepted April 20, 2014; published online October 17, 2014

Tuite has been suggested as a potential reservoir for trace elements in the deep mantle, but no evidence confirms this supposition. By using a natural apatite as starting material, the trace-element-bearing tuite large crystals were obtained under high-pressure and high-temperature conditions (15 GPa and 1800 K). X-ray diffraction pattern and Micro-Raman spectrum of the run product confirm that tuite was synthesized. The concentrations of trace elements in tuite crystals were analyzed by laser ablation-inductively coupled plasma-mass spectrometry (LA-ICP-MS). The rare earth element patterns of tuite show enrichment of light rare earth elements relative to heavy rare earth elements. Tuite shows high concentrations of Th and Sr, and negative anomalies of Rb, Nb, and Hf. The results show that tuite can accommodate a large amount of trace elements. Tuite might be an important host to accommodate trace elements if there is much apatite subducted into the deep mantle.

tuite, trace elements, high-pressure and high-temperature

Citation: Zhai S M, Xue W H, Yamazaki D, et al. 2014. Trace element composition in tuite decomposed from natural apatite in high-pressure and high-temperature experiments. Science China: Earth Sciences, 57: 2922−2927, doi: 10.1007/s11430-014-4980-7

Apatite is a common accessory mineral in igneous, metamorphic and sedimentary rocks on earth and in lunar rocks as well as meteorites (Nash, 1984). It is also a major host for rare earth elements (REE) and large ion lithophile elements (LILE) (such as U, Th, Ba, Sr) in almost all igneous and metamorphic rocks (Griffin et al., 1972; Beswick and Carmichael, 1978; Jolliff et al., 1993). Experimental results show that apatite is not stable at high-pressure and high-temperature conditions (Murayama et al., 1986). Hydroxyapatite and fluorapatite decompose at ~13 GPa and 1000°C, and one of the decomposed products was γ-$Ca_3(PO_4)_2$, which was first discovered in Suizhou L6 chondrite and named as tuite (Xie et al., 2002, 2003; Xie and Chen, 2008). Later tuite was also found in other chondritic and SNC meteorites (Ozawa et al., 2007; Greshake and Fritz, 2009; Miyahara et al., 2011; Baziotis et al., 2013). On the other hand, tuite was believed as a high-pressure polymorph of whitlockite with structure identical to that of synthetic β-$Ca_3(PO_4)_2$ (Gopal and Calvo, 1972; Prewitt and Rothbard, 1975; Dowty, 1977). According to previous studies, apatite and whitlockite can contain a large amount of REE, even up to 11.4% (Puchelt and Emmermann, 1976) and 13% (Jolliff et al., 1993), respectively. Therefore, tuite might have a significant implication for REE since it is a decomposed product of apatite and the high-pressure polymorph of whitlockite.

In mineral structure of tuite, a phosphorus atom is tetrahedrally coordinated by oxygen atoms and calcium atoms occupy two types of large cation sites. The 12-coordinated

*Corresponding author (email: zhaishuangmeng@vip.gyig.ac.cn)

Ca(1) has a mean bond length of 0.2739 nm and 10-coordinated Ca(2) has a mean bond length of 0.2588 nm (Sugiyama and Tokonami, 1987). These mean bond lengths are larger than those of 8-coordinated Ca sites in garnet and diopside (about 0.240 nm for Ca–O bond) (Xie et al., 2003). Therefore, tuite was thought to be a potential accommodation for REE and LILE in the deep upper mantle (>400 km) (Murayama et al., 1986; Sugiyama and Tokonami, 1987; Xie et al., 2003). Two recent studies on 10 trace elements (including Nb, Ta, Zr, Y, Ba, Sr, Rb, Ce, Nd and Lu) doped in apatite-silicate systems were reported and a few rare earth elements (including Y, Ce, Nd and Lu) in tuite were analyzed (Konzett and Frost, 2009; Konzett et al., 2012). The reported hydroxyapatite-MORB and apatite-peridotite systems are complicated and important for understanding of apatite in silicate system (Konzett and Frost, 2009; Konzett et al., 2012). But the fundamental information, e.g., the concentration of trace elements in tuite formed from natural apatite, is also important. The grain size of tuite was quite small (less than 30 μm) in their studies, and the content of trace elements were analyzed by electron microprobe analyzer (EPMA) (Konzett and Frost, 2009; Konzett et al., 2012). In fact, the laser ablation-inductively coupled plasma-mass spectrometry (LA-ICP-MS) is a powerful method to analyze the concentrations of trace elements in minerals (Jackson et al., 1992). So far there is no report about the rare earth elements and other trace elements in large tuite crystal analyzed by LA-ICP-MS.

In hydroxyapatite-MORB system, synthetic hydroxyapatite was included and only 10 trace elements were doped (Konzett and Frost, 2009). In the present study, we used a natural apatite sample containing many trace elements as starting material to carry out high-pressure and high-temperature experiment. We first obtained large tuite cystals, which were identified by X-ray diffraction and Micro-Raman spectrum. The concentrations of trace elements in tuite were analyzed by LA-ICP-MS. Based on the concentrations of trace elements, tuite might be an important host to accommodate trace elements if much apatite decomposes in the deep mantle (>400 km).

1 Experimental and analytical methods

The natural apatite sample used in this study is one of the major mineral phases in Eppawala carbonatites, Sri Lanka. The details of the apatite were described by Manthilake et al. (2008). In this study, powder apatite sample with chemical compositions shown as second column under Aptite>Eppawala in Table 1 of Manthilake et al. (2008) was used as starting material for synthesis of tuite. The powder sample is core part without inclusions of large apatite crystal.

High-pressure and high-temperature experiment was performed at 15 GPa and 1800 K for 24 h using a 1000-ton Kawai-type multi-anvil apparatus (USSA-1000) installed at Institute for Study of the Earth's Interior, Okayama University. Tungsten carbide cubes with edge length of 32 mm and truncated edge length (TEL) of 4.0 mm were employed for the second stage anvils. A semi-sintered octahedron with 10 mm edge length made of 95 wt% MgO+5 wt% Cr_2O_3 was used as a pressure medium with pyrophyllite gaskets. A $LaCrO_3$ cylindrical heater was put in a ZrO_2 thermal insulating tube. A thin graphite capsule was used as a sample chamber. The quenching method was adopted in the experiment. Some large synthetic single crystals (200–350 μm) were selected from the recovered sample and mounted in epoxy for polishing. The polished crystals were identified by microfocused X-ray diffractometer (RINT RAPID II-CMF) equipped with a rotating Cu anode operated at 1.2 kW, and the chemical compositions were examined by electron probe micro analyzer (JXA-8800) operated at 15 kV and 12 nA.

Trace elements in recovered crystals were determined from polished section using a laser ablation-inductively coupled plasma-mass spectrometry (LA-ICP-MS) at Peking University. The LA-ICP-MS system consists of a COMPexPRO excimer laser linked to the Agilent 7500cs ICP-MS. The laser was operated at 193 nm wavelength with 15 mJ energy, 5 Hz frequency. The laser beam was condensed with a beam expander and shaped with an adjustable iris aperture to produce a crater size of 60 μm on the sample surface. Ablation duration was usually about 75 s and was done in pure He atmosphere. The first 15 s of acquisition were used to measure the gas blank followed by about 60 s of acquiring a mixture of gases and ablated materials. We used the following gas flows: He, 500 mL/min; Ar carrier, 0.96 L/min; Ar plasma, 15 L/min. Plasma RF was 1550 W. NIST 610 glass standards reported by Pearce et al. (1997) were used for calibrations of relative sensitivities. Each analysis was normalized using the CaO content of tuite determined by electron microprobe. NIST 612 and 614 glasses were used as external standards. Trace-element reductions were done with the GLITTER software (Van Achterberg et al., 2001).

2 Results and discussion

The typical X-ray pattern and Raman spectrum of synthetic single crystal was shown in Figure 1, which confirms that the synthetic product is tuite. All X-ray peaks as shown in Figure 1(a) can be attributed to rhombohedral γ-$Ca_3(PO_4)_2$ (space group: *R*-3*m*). The X-ray pattern was collected from a polished section of a single crystal and the relative intensities of peaks are different from previous studies of tuite (Zhai et al, 2009, 2010). The Raman spectrum shown in Figure 1(b) indicates typical bands of 414, 578, 643, 976, 1003 and 1094 cm^{-1}, which are consistent with previous studies of natural and synthetic tuite (Xie et al., 2003; Zhai et al., 2010, 2011).

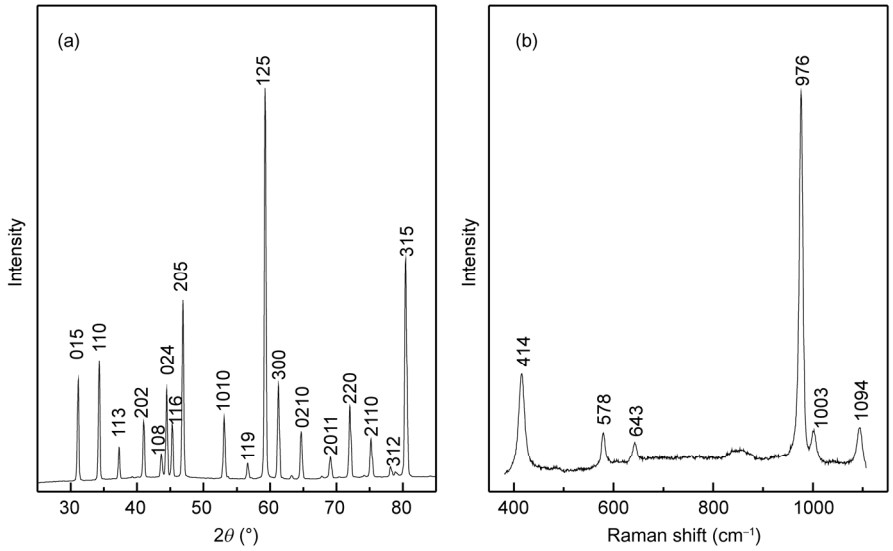

Figure 1 Represetative X-ray diffraction pattern (a) and Raman spectrum (b) of synthetic tuite in this study.

Table 1 Chemical composition of synthetic tuite crystals[a)]

Major element (wt%)	Tu-1*	Tu-2*	Tu-3*	Tu-4*	Tuite**	Apatite (Manthilake et al., 2008)
SiO_2	0.12	0.16	0.09	0.15	–	2.39
Al_2O_3	0.01	0.01	0.01	0.01	–	0.05
FeO	0.03	0.01	0.01	0.01	0.38	0.05
MnO	0.04	0.03	0.04	0.04	–	0.02
MgO	0.21	0.23	0.20	0.21	3.58	0.27
CaO	52.56	53.08	53.14	52.51	46.14	54.35
P_2O_5	45.81	45.72	46.13	45.50	47.16	42.45
LOI						0.53
Total	98.78	99.24	99.62	98.43	100.22	100.04

a) *, the chemical compositions of each tuite crystal were averaged values of five measurements. **, in natural tuite reported by Xie et al. (2003), there are some other components including Na_2O, K_2O, NiO and TiO_2

The chemical compositions of tuite are listed in Table 1. Compared with the chemical compositions of apatite starting material reported by Manthilake et al. (2008) and natural tuite in Suizhou L6 chondrite reported by Xie et al. (2003), tuite is poor with SiO_2, indicating that the solubility of SiO_2 in tuite is quite low. In order to check the possible OH, F and Cl in synthesized tuite, the samples were analyzed by Raman spectroscopy and energy dispersive spectrum analysis (EDS). No evidence shows the existence of OH or F. But the EDS analysis shows the evidence of Cl with 0.35 wt%–0.94 wt%, and gives an average of 0.65 wt% for 31 points. The EDS analysis may have great uncertainty, but it can show the existence of Cl.

Depending on the sizes of tuite single crystals, three to five pits were analyzed by LA-ICP-MS, as shown in Figure 2. The trace-element abundances in tuite are listed in Table 2.

According to decomposed reaction of apatite and mass balance, the abundances of trace elements in tuite should be higher than those in apatite starting material if we suppose tuite accommodates all trace elements after the decomposition of apatite. But the present results show that the corresponding concentration of trace element is generally lower than that of apatite starting material. The decomposed products of apatite may include CaF_2, CaO and liquid, which may accommodate a part of trace elements. Previous studies showed that REE are significantly enriched in many fluorites (Bau and Dulski, 1995; Grammaccioli et al., 1999; Schwinn and Markl, 2005). The CaF_2 phase might accommodate some amount of REE, which is another issue to be investigated in the future. Since in the decomposed products the CaF_2 is quite small in volume or weight percentage, it is difficult to find such small phase in enough size for LA-ICP-MS measurement.

The concentrations of La in tuite are much higher than those of apatite starting material. We used a thin graphite capsule as a sample chamber, and graphite transferred to diamond at the experimental conditions. A $LaCrO_3$ heater was set outside of the capsule; therefore, a small part of $LaCrO_3$ may penetrate the capsule at high-temperature and retains in the sample, which causes higher concentration of La and Cr in the sample. Based on the results, we can conclude that tuite can accommodate a large amount of La

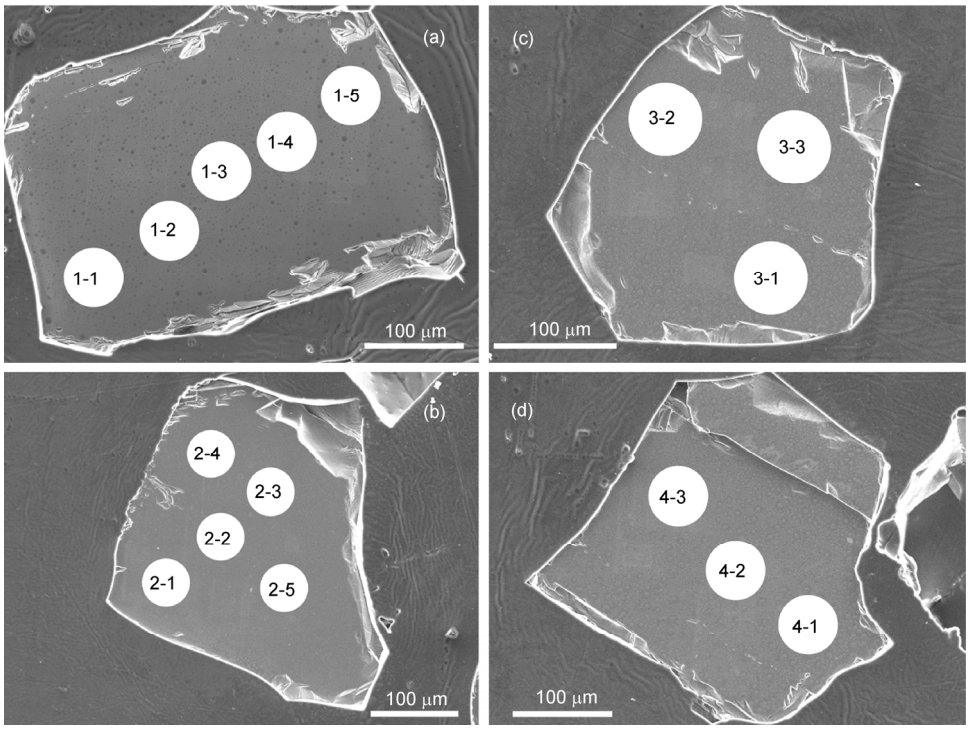

Figure 2 Backscattered-electron images of the synthetic tuite crystals. The circles represent LA-ICP-MS analyzed pits with diameter of 60 μm.

Table 2 Trace-element concentrations (ppm) in synthetic tuite crystals shown in Figure 2

	1-1	1-2	1-3	1-4	1-5	2-1	2-2	2-3	2-4	2-5	3-1	3-2	3-3	4-1	4-2	4-3	Average
Rb	0.14	0.13	0.14	0.15	0.17	0.24	0.19	0.13	0.27	0.10	0.11	0.22	0.17	0.26	0.25	0.25	0.18
Sr	3133	3066	3023	3053	2980	3091	3083	3142	3148	3065	3127	3147	3142	2945	2964	3007	3070
Y	55.6	54.1	52.8	53.0	50.1	52.3	55.3	58.7	55.5	56.2	54.7	52.5	55.6	50.3	49.9	48.2	53.4
Zr	9.9	14.1	13.5	14.0	11.2	9.8	10.8	12.9	9.9	10.8	11.5	10.7	11.8	10.6	10.9	9.9	11.4
Nb	0.63	0.50	0.25	0.50	0.56	0.46	0.56	0.58	0.41	0.58	0.61	0.53	0.56	0.60	0.56	0.57	0.53
Cs	0.08	0.08	0.08	0.09	0.10	0.10	0.08	0.07	0.12	0.06	0.10	0.13	0.09	0.11	0.08	0.11	0.09
Ba	79.7	80.3	80.2	81.9	82.3	86.4	82.5	77.1	90.6	76.1	75.9	83.9	81.2	91.1	94.9	85.9	83.1
La	16633	17341	18695	19031	20865	20646	18022	14213	20903	14422	14169	19159	16942	18682	25775	23364	18679
Ce	845.4	785.9	739.6	728.4	644.9	568.4	678.1	864.5	613.7	843.7	870.4	709.5	791.0	715.4	748.9	752.9	743.8
Pr	102.6	94.8	80.4	88.3	78.4	68.2	81.6	102.7	74.2	101.5	104.7	85.7	94.6	93.8	90.9	87.0	89.3
Nd	441.3	415.1	394.2	389.9	343.5	293.4	353.3	441.0	319.1	437.9	452.7	369.4	404.7	383.8	368.4	373.2	386.3
Sm	63.9	59.9	56.9	56.3	50.5	42.7	52.2	63.5	46.6	63.1	64.7	53.4	58.6	55.9	57.2	54.8	56.3
Eu	12.5	11.8	11.2	11.1	10.1	9.3	10.5	12.6	9.9	12.3	12.6	10.9	11.6	11.6	10.9	10.9	11.2
Gd	35.6	34.0	32.9	32.1	29.1	24.7	29.6	35.6	27.3	35.7	36.3	30.2	32.6	32.8	31.6	31.2	32.0
Tb	3.14	2.96	2.85	2.81	2.49	2.17	2.57	3.09	2.35	3.14	3.15	2.62	2.83	2.68	2.79	2.66	2.77
Dy	12.5	11.8	11.4	11.1	10.1	9.2	10.5	12.6	9.8	12.4	12.5	10.7	11.5	10.8	10.1	10.9	11.1
Ho	1.98	1.91	1.85	1.83	1.70	1.54	1.73	1.95	1.65	1.97	1.97	1.75	1.85	1.59	1.59	1.63	1.78
Er	4.48	4.39	4.36	4.36	4.16	3.94	4.19	4.63	4.15	4.51	4.55	4.34	4.38	4.28	4.18	4.12	4.31
Tm	0.58	0.56	0.57	0.57	0.57	0.56	0.55	0.57	0.56	0.57	0.56	0.56	0.58	0.56	0.58	0.57	0.57
Yb	3.86	3.77	3.81	3.95	3.92	3.86	3.79	3.77	3.96	3.69	3.69	3.98	3.85	3.72	3.93	3.85	3.84
Lu	0.63	0.63	0.65	0.68	0.67	0.67	0.66	0.62	0.70	0.61	0.59	0.67	0.63	0.65	0.69	0.67	0.65
Hf	0.13	0.21	0.20	0.21	0.16	0.14	0.15	0.20	0.11	0.35	0.19	0.15	0.14	0.14	0.16	0.17	0.18
Ta	0.37	0.23	0.07	0.25	0.31	0.21	0.26	0.29	0.20	0.28	0.35	0.28	0.30	0.33	0.32	0.35	0.28
Th	15.1	14.0	13.5	12.1	9.8	10.0	16.4	24.1	10.0	13.3	19.6	13.1	20.1	13.4	12.0	12.5	14.3
U	0.32	0.33	0.31	0.27	0.26	0.24	0.32	0.44	0.25	0.47	0.37	0.27	0.29	0.29	0.30	0.29	0.31
Cr	404.4	418.8	414.4	432.8	426.0	348.3	348.4	354.6	337.4	345.5	449.0	396.5	527.3	435.5	430.0	425.7	405.9

(more than 2 wt%).

The averaged concentrations of trace elements in each crystal are chondrite-normalized for REE, shown in Figure 3. The chondrite and pyrolitic mantle values reported by McDonough and Sun (1995) are adopted to normalize the concentrations of trace elements in this study. The REE patterns of four tuite crystals illustrated in Figure 3(a) are similar, and show enrichment of light rare earth elements relative to heavy rare earth elements. The distribution of trace elements in tuite plotted in Figure 3(b) shows negative Rb, Nb, and Hf anomalies due to their concentrations in apatite starting material, and higher concentrations of REE and LILE (e.g., Th, Sr). Due to the same charge and preferred coordination geometry and small difference in the radii of cation, Sr can substitute Ca in the γ-$Ca_3(PO_4)_2$ (Zhai et al., 2010).

The concentrations of REE in tuite are 2 to 3 order higher than those in garnets and pyroxenes reported in literature (Zheng et al., 2005; Python et al., 2007; Gaspar et al., 2008; Zhang et al., 2009; Dégi et al., 2010; Santosh et al., 2010). However, the amount of tuite is far smaller compared with the major silicate mineral phases, such as garnet and pyroxene, in the subducted MORB (Konzett and Frost, 2009). On the other hand, there is no information about the partitioning coefficients between tuite and garnet or pyroxene. Therefore, it is difficult to determine how much REE tuite

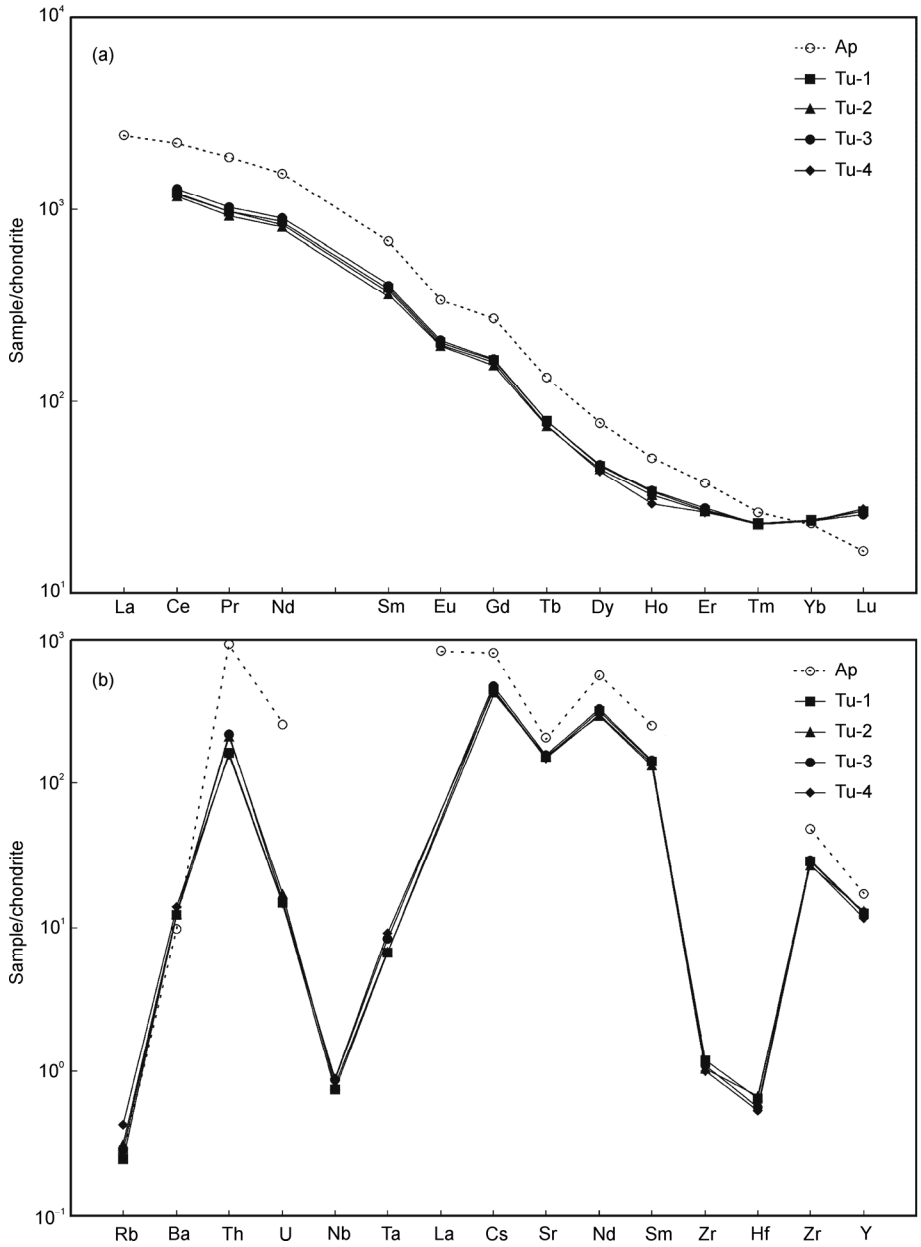

Figure 3 Chondrite-normalized averaged REE patterns (a) and primitive mantle-normalized other trace-element abundances (b) of synthetic tuite crystals (Tu-1, Tu-2, Tu-3, Tu-4) and starting material (Ap). The chondrite values are from McDonough and Sun (1995).

can accommodate in coexisting silicate minerals assemblage. Much more information about these issues needs to be investigated.

3 Conclusions

Obviously the present results confirm that tuite can accommodate large amounts of REE and LILE, which is of geochemical significance. Tuite is the high-pressure polymorph of whitlockite and one of the decomposed products of apatite, and stable at least in the upper mantle. Therefore, tuite might be an important host for accommodation of trace elements in the deep mantle. The uptake of trace elements in tuite is another uncovered issue. And the partitioning coefficients of trace elements between tuite and silicate minerals, such as garnet and pyroxenes, also are required for understanding the behaviors of trace elements in the deep mantle.

The natural trace-element-bearing apatite sample used in this study was kindly provided by Dr. Geeth Manthilake. We thank Shan Shuangming and Guo Xinzhuan for their helps with the high-pressure and high-temperature experiment and SEM observation. The LA-ICP-MS analysis was performed at Peking University with helps from Sun Yi. Cheng Hao, Liu Shuwen and Ito Eiji are thanked for helpful discussion. This work was financially supported by National Natural Science Foundation of China (Grant No. 40973045).

Bau M, Dulski P. 1995. Comparative study of yttrium and rare-earth element behaviours in fluorine-rich hydrothermal fluids. Contrib Mineral Petrol, 119: 213–223

Baziotis I P, Liu Y, DeCarli P S, et al. 2013. The Tissint Martian meteorite as evidence for the largest impact excavation. Nat Commun, 4: 1404

Beswick A E, Carmichael I S E. 1978. Constrains on mantle source compositions imposed by phosphorous and the rare earth elements. Contrib Mineral Petrol, 67: 317–330

Dégi J, Abart R, Török K. 2010. Symplectite formation during decompression induced garnet breakdown in lower crustal mafic granulite xenoliths: Mechanisms and rates. Contrib Mineral Petrol, 159: 293–314

Dowty E. 1977. Phosphate in Angra dos Reis: Structure and composition of the $Ca_3(PO_4)_2$ minerals. Earth Planet Sci Lett, 35: 347–351

Gaspar M, Knaack C, Meinert L D, et al. 2008. REE in skarn systems: A LA-ICP-MS study of garnets from the Crown Jewel gold deposit. Geochim Cosmochim Acta, 72: 185–205

Gopal R, Calvo C. 1972. Structure relationship of whitlockite and β-$Ca_3(PO_4)_2$. Nat Phys Sci, 237: 30–32

Grammaccioli C M, Diella V, Demartin F. 1999. The role of fluoride complexes in REE geochemistry and the importance of 4f electrons: Some examples in minerals. Eur J Mineral, 11: 983–992

Greshake A, Fritz J. 2009. Discovery of ringwoodite, wadsleyite, and γ-$Ca_3(PO_4)_2$ in Chassigny: Constraints on shock conditions. Lunar Planet Inst Sci Conf Abs, 40: 1586

Griffin W L, Åmli R, Heier K S. 1972. Whitlockite and apatite from lunar rock 14310 and from ÖdegÅrden, Norway. Earth Planet Sci Lett, 15: 53–68

Jackson S E, Longerich H P, Dunning G R, et al. 1992. The application of laser-ablation microprobe; inductively coupled plasma-mass spectrometry (LAM-ICP-MS) to *in situ* trace-element determinations in minerals. Can Mineral, 30: 1049–1064

Jolliff B L, Haskin L A, Colson R O, et al. 1993. Partitioning in REE-saturating minerals: Theory, experiment, and modeling of whitlockite, apatite, and evolution of lunar residual magmas. Geochim Cosmochim Acta, 57: 4069–4094

Konzett J, Frost D J. 2009. The high *P-T* stability of hydroxyl-apatite in natural and simplified MORB—An experimental study to 15 GPa with implications for transport and storage of phosphorus and halogens in subduction zones. J Petrol, 50: 2043–2062

Konzett J, Rhede D, Frost D J. 2012. The high PT stability of apatite and Cl partitioning between apatite and hydrous potassic phases in peridotite: An experimental study to 19 GPa with implications for the transport of P, Cl and K in the upper mantle. Contrib Mineral Petrol, 163: 277–296

Manthilake M A G M, Sawada Y, Sakai S. 2008. Genesis and evolution of Eppawala carbonatites, Sri Lanka. J Asian Earth Sci, 32: 66–75

McDonough W F, Sun S. 1995. The composition of the Earth. Chem Geol, 120: 223–253

Miyahara M, Ohtani E, Ozawa S, et al. 2011. Natural dissociation of olivine to (Mg, Fe)SiO_3 perovskite and magnesiowüstite in a shocked Martian meteorite. Proc Natl Acad Sci USA, 108: 5999–6003

Murayama J K, Nakai S, Kato M, et al. 1986. A dense polymorph of $Ca_3(PO_4)_2$: A high pressure phase of apatite decomposition and its geochemical significance. Phys Earth Planet Inter, 44: 293–303

Nash W P. 1984. Phosphate minerals in terrestrial igneous and metamorphic rocks. In: Nriagu J O, Moore P B, eds. Phosphate Minerals. Berlin: Springer-Verlag. 215–241

Pearce N J G, Perkins W T, Westgate J A, et al. 1997. A compilation of new and published major and trace element data for NIST SRM 610 and NIST SRM 612 glass reference materials. Geostand Newsl, 21: 115–144

Prewitt C T, Rothbard D R. 1975. Crystal structures of meteoritic and lunar whitlockites. Lunar Planet Sci, 6: 646–648

Puchelt H, Emmermann R. 1976. Bearing of rare earth patterns of apatites from igneous and metamorphic rocks. Earth Planet Sci Lett, 31: 279–286

Python M, Ishisa Y, Ceuleneer G, et al. 2007. Trace element heterogeneity in hydrothermal diopside: Evidence for Ti depletion and Sr-Eu-LREE enrichment during hydrothermal metamorphism of mantle harzburgite. J Mineral Petrol Sci, 102: 143–149

Ozawa S, Ohtani E, Suzuki A, et al. 2007. Shock metamorphism of L6 chondrites Sahara 98222 and Yamato 74445: The *P-T* conditions and the shock age. AGU Fall Meet Abs, 1: 1234

Santosh M, Rajesh V J, Tsunogae T, et al. 2010. Diopsidites from a Neoproterozoic-Cambrian suture in southern India. Geol Mag, 147: 777–788

Schwinn G, Markl G. 2005. REE systematics in hydrothermal fluorite. Chem Geol, 216: 225–248

Sugiyama K, Tokonami M. 1987. Structure and crystal chemistry of a dense polymorph of tricalcium phosphate $Ca_3(PO_4)_2$: A host to accommodate large lithophile elements in the Earth's mantle. Phys Chem Miner, 15: 125–130

Van Achterberg E, Ryan C G, Jackson S, et al. 2001. Data reduction software for LA-ICP-MS. In: Sylvester P, ed. Laser-Ablation-ICPMS in the Earth Sciences: Principles and Applications. Mineralogical Society of Canada. 239–243

Xie X, Chen M. 2008. Formation conditions of tuite (in Chinese). Geochimica, 37: 297–303

Xie X, Minitti M E, Chen M, et al. 2002. Natural high-pressure polymorph of merrillite in the shock veins of the Suizhou meteorite. Geochim Cosmochim Acta, 66: 2439–2444

Xie X, Minitti M E, Chen M, et al. 2003. Tuite, γ-$Ca_3(PO_4)_2$: A new mineral from the Suizhou L6 chondrite. Eur J Mineral, 15: 1001–1005

Zhai S, Liu X, Shieh S R, et al. 2009. Equation of state of γ-tricalcium phosphate, to lower mantle pressures. Am Mineral, 94: 1388–1391

Zhai S, Wu X, Ito E. 2010. High-pressure Raman spectra of tuite, γ-$Ca_3(PO_4)_2$. J Raman Spectrosc, 41: 1011–1013

Zhai S, Xue W, Lin C, et al. 2011. Raman spectra and *X*-ray diffraction of tuite at various temperatures. Phys Chem Miner, 38: 639–646

Zhang R Y, Liou J G, Zheng J P, et al. 2009. Petrogenesis of eclogites enclosed in mantle-derived peridotites from the Sulu UHP terrane: Constraints from trace elements in minerals and Hf isotopes in zircon. Lithos, 109: 176–192

Zheng J P, Zhang R Y, Griffin W L, et al. 2005. Heterogeneous and metasomatized mantle recorded by trace elements in minerals of the Donghai garnet peridotites, Sulu UHP terrane, China. Chem Geol, 221: 243–259